Title

Variation in Rapa Nui (Easter Island) land use indicates production and population peaks prior to European contact

Journal

Proceedings of the National Academy of Sciences of the United States of America, 112(4)

ISSN

0027-8424

Authors

Stevenson, Christopher M
Puleston, Cedric O
Vitousek, Peter M
et al.

Publication Date

2015-01-27

DOI

10.1073/pnas.1420712112

Peer reviewed

Variation in Rapa Nui (Easter Island) land use indicates production and population peaks prior to European contact

Christopher M. Stevenson[a,1], Cedric O. Puleston[b], Peter M. Vitousek[c], Oliver A. Chadwick[d], Sonia Haoa[e], and Thegn N. Ladefoged[f,g]

[a]Anthropology Program, School of World Studies, Virginia Commonwealth University, Richmond, VA 23284; [b]Department of Anthropology, University of California, Davis, CA 95616; [c]Department of Biology, Stanford University, Stanford, CA 94305; [d]Department of Geography, University of California, Santa Barbara, CA 93106; [e]Fundación Mata Ki Te Rangi, Hanga Roa, Rapa Nui, Chile; and [f]Te Pūnaha Matatini and [g]Department of Anthropology, University of Auckland, Auckland, New Zealand 1142

Edited by Patrick V. Kirch, University of California, Berkeley, CA, and approved December 12, 2014 (received for review October 29, 2014)

Many researchers believe that prehistoric Rapa Nui society collapsed because of centuries of unchecked population growth within a fragile environment. Recently, the notion of societal collapse has been questioned with the suggestion that extreme societal and demographic change occurred only after European contact in AD 1722. Establishing the veracity of demographic dynamics has been hindered by the lack of empirical evidence and the inability to establish a precise chronological framework. We use chronometric dates from hydrated obsidian artifacts recovered from habitation sites in regional study areas to evaluate regional land-use within Rapa Nui. The analysis suggests region-specific dynamics including precontact land use decline in some near-coastal and upland areas and postcontact increases and subsequent declines in other coastal locations. These temporal land-use patterns correlate with rainfall variation and soil quality, with poorer environmental locations declining earlier. This analysis confirms that the intensity of land use decreased substantially in some areas of the island before European contact.

Rapa Nui | population | obsidian | dating | collapse

There is ongoing debate about the demographic trajectory of Rapa Nui (or Easter Island) from its settlement around AD 1200 (1–4) until the arrival of Jesuit missionaries in the 1860s (Fig. 1) (5). The central issue is whether the Rapa Nui population experienced significant demographic decline before European contact in AD 1722. Proponents of this "pre-contact collapse" scenario suggest that environmental degradation reduced food production, and a number of researchers have elaborated a chronological model (6) that argues for a period of warfare, population reduction, and political fragmentation in the AD 1500s (7–13) or late AD 1600s (14–16). Alternately, other researchers view the archaeological evidence as favoring sociopolitical continuity until Western smallpox, syphilis, and tuberculosis pathogens decimated the population after European contact (17–22).

There is archaeological evidence for societal change on Rapa Nui, including the manufacture of obsidian spear points, the destruction of elite dwellings, habitation in refuge caves, cannibalism, a change in burial practice, and a marked ideological shift away from ceremonial platform (*ahu*) structures to the formation of the Birdman (*tangata manu*) cult centered at Orongo (see ref. 23 for a summary). These changes have been associated with the abandonment of inland field systems and houses and decreased population levels (14–16, 24). The question is when these changes occurred. Poor chronological control over the timing of past events in all these cases makes it difficult to draw firm conclusions as to whether these changes occurred before or after European contact. Oral histories recorded in the early 20th century by Routledge (25) reflect a period of precontact societal upheaval but are shrouded in mythology.

Empirical evidence for societal collapse, extensive environmental degradation (other than deforestation), or warfare that could have caused such a collapse before European contact is minimal (20). A recent analysis of radiocarbon dates from throughout Rapa Nui noted the inherent (and severe) ambiguities in radiocarbon calibrations in the time period of interest but concluded that there was demographic continuity into the postcontact era as opposed to population decline during the late precontact period (19). Additional analysis of ^{14}C and obsidian hydration dates from a smaller study region in Hanga Ho'onu on the northeast coast also reported continuity of settlement and agricultural activity into the period of European contact (18). For environmental degradation, there is substantial evidence for deforestation (26–30) but its timing and causes have been debated (2, 31–34). Soil erosion occurred in limited areas (i.e., on the older Poike peninsula (35–37), along a small section of the northwest coast, and on the slopes of some of the smaller volcanic cones); however, there is no evidence of widespread soil erosion that could have interfered with agricultural production (38). The assertion that the proliferation of obsidian spear points is an indicator of endemic violence is challenged by lithic use-wear analysis that shows the artifacts to be used extensively in processing vegetation (39, 40).

Here we identify spatial and temporal variation in the intensity of land use across portions of Rapa Nui and relate these observations

Significance

Our paper evaluates a long-standing debate and examines whether the prehistoric population of Rapa Nui experienced a significant demographic collapse prior to European contact in AD 1722. We have used dates from hydrated obsidian artifacts recovered from habitation sites as a proxy for land use over time. The analysis suggests region-specific dynamics that include the abandonment of leeward and interior locations. These temporal land-use patterns correlate with rainfall variation and soil quality. This analysis demonstrates that the concept of "collapse" is a misleading characterization of prehistoric human population dynamics. As a result, we see our approach as useful in the study of other prehistoric societies for which a sudden demographic collapse has been proposed in prehistory.

Author contributions: C.M.S., P.M.V., O.A.C., S.H., and T.N.L. designed research; C.M.S., P.M.V., O.A.C., S.H., and T.N.L. performed research; C.O.P. contributed new reagents/analytic tools; C.M.S., C.O.P., P.M.V., O.A.C., and T.N.L. analyzed data; and C.M.S., C.O.P., P.M.V., O.A.C., and T.N.L. wrote the paper.

The authors declare no conflict of interest.

This article is a PNAS Direct Submission.

[1]To whom correspondence should be addressed. Email: cmstevenson@vcu.edu.

This article contains supporting information online at www.pnas.org/lookup/suppl/doi:10.1073/pnas.1420712112/-/DCSupplemental.

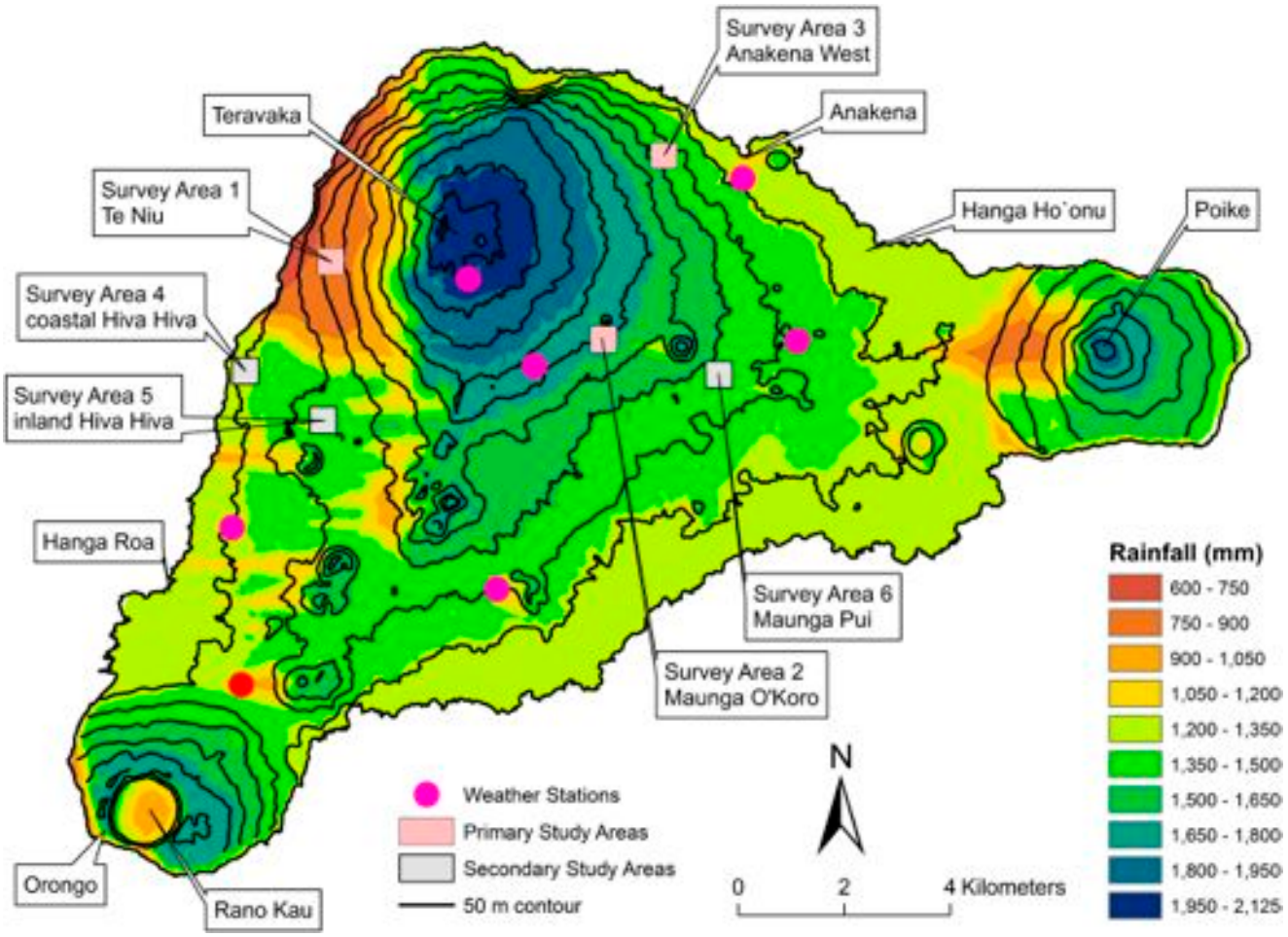

Fig. 1. A map of Rapa Nui showing the three study areas (pink squares) and locations mentioned in the text. Rainfall isohyets demonstrate the rain shadow effect. Note that the area in the northwest of the island appears to be quite dry, as does the area immediately west of Poike, the peninsula on the extreme east of the island. Both these areas are, in fact, drier than elevation alone would predict. Solid purple dots represent field weather stations. The red dot represents the weather station at the Mataveri airport.

to new data on spatial variation in climate and soil fertility. We base our analysis of land use on obsidian hydration dating (OHD) of tools and flakes, using 428 obsidian hydration dates developed under revised calibrations and protocols (*SI Appendix*, Table S1) (41, 42). Obsidian nodules were fashioned into everyday working tools and are plentiful at many archaeological sites. We use the quantity of hydration dates as a measure of the amount of discarded material over time and as a proxy for land-use intensity.

The Rapa Nui Environment and Study Areas

The island of Rapa Nui was created by multiple volcanic events (43). Early eruptions formed the spatially separate Poike (0.78–0.36 Mya), Rano Kau (0.78–0.34 Mya), and Maunga Terevaka (0.77–0.30 Mya) volcanos. Between 0.24–0.11 Mya additional eruptions from M. Terevaka joined the three land masses and formed the land surface upon which ancient agriculture was later practiced. M. Terevaka reaches a height of 505 m, with annual rainfall increasing with elevation. However, there is a well-defined rain shadow on the northwest coast in the area known as Te Niu (Fig. 1). Our recent recording and analysis of climatic data (Table 1 and see *SI Appendix*, Table S3) suggests that rainfall ranges from *ca*. 2,100 mm/y at the top of M. Terevaka to a low of *ca*. 630 mm/y along the coast in the rain shadow. Analysis of modern rainfall data from 1958–1997 shows considerable year-to-year variation, with droughts occurring (17). Our climatic data show that near-surface annual soil temperatures also are elevation dependent and average 22–24 °C on the coastal plain and 19 °C just below the summit of M. Terevaka (*SI Appendix*, Fig. S1 and Table S2).

Soil properties related to soil fertility vary substantially across Rapa Nui, reflecting variation in climate, age of the volcanic substrate, and topography (44, 45). Differential rainfall has caused substantial variation in Rapa Nui soil nutrients, as it does in volcanic substrates of similar age in Hawai'i (46, 47), and older substrates generally are depleted in soil nutrients compared with younger ones. Although soils of the lowland areas with moderate rainfall are richer in biologically available nutrients than are wetter, higher elevation soils (45), all but the richest Rapa Nui soils are nutrient depleted in comparison with the soils where precontact Hawaiian farmers intensified agricultural production (48). On Rapa Nui, the primary cultigens were sweet potato (*Ipomoea batatas*), dryland taro (*Colocasia esculenta*), yam (*Dioscorea* spp.), and ti (*Cordyline*) (49), of which sweet potato was perhaps a secondary introduction (50). Within several centuries after settlement, beginning about AD 1400, these crops became intensively cultivated in lithic mulch gardens (49, 51). Recent analysis of modern rainfall data documents periodic droughts, and if similar conditions existed earlier in time (52), such climatic events would have affected crop production, with taro being

Table 1. Location of study areas with corresponding distance to coast, elevation, rainfall values (measurements taken at the center of a 500 × 500 m quadrant), and soil nutrient properties

Study area	Distance to coast, m	Elevation, m	Rainfall*, mm	Resin phosphorus†, mean (SD), mg/kg	Exchangeable calcium‡, mean (SD), cmol(+)/kg	Base saturation§, mean (SD), %	n¶
SA1	860	120	805	4.26 (8.28)	6.03 (3.56)	16.26 (10.60)	58
SA2	4,340	260	1,690	0.49 (0.62)	0.82 (0.57)	2.89 (1.89)	31
SA3	792	170	1,460	14.6 (24.88)	4.42 (3.09)	14.76 (6.73)	71

*Rainfall estimated based on an orographic and wind direction rainfall model by Puleston (*SI Appendix, Text*).
†Phosphorus measured with an anion exchange resin to identify plant-available phosphate.
‡Calcium extracted from the soil cation exchange complex to identify plant-available Ca^{2+}.
§The percentage of Ca^{2+}, Mg^{2+}, Na^{+}, and K^{+} on the soil cation exchange complex is used as a measure of soil fertility because calcium, magnesium, and potassium are plant nutrients.
¶Number of discrete samples taken at 20- to 25- or 0- to 30-cm depth increments inside and outside garden areas with identifiable garden features.

most vulnerable and sweet potato being more resilient to the parameters of the island's fluctuating rainfall (17).

We evaluated region-specific land-use patterns in six study areas on Rapa Nui, focusing on three for which we have information on climate, soils, and land-use trends derived from numerous obsidian hydration dates (Fig. 1 and Table 1). The three intensive study areas were situated to sample diverse environmental settings. Study Area 1 (SA1) is located near the northwest coast at a low-rainfall site in the rain shadow of M. Terevaka. SA2 is located in the interior on the slopes of M. Terevaka at a distance of more than 4 km from the southern coast and is a higher-elevation, high-rainfall location. SA3 is located just inland on the northeast coast, west of Anakena beach. SA1 has relatively high soil nutrient availability as indexed by plant-available phosphorus, calcium, and base saturation but low rainfall; SA2 has the lowest nutrient supply and highest rainfall; and SA3 is characterized by intermediate amounts of rainfall and relatively high soil nutrient levels (Table 1). The other three regions that we sampled on Rapa Nui are located in Fig. 1, and their properties are summarized in *SI Appendix*, Table S3.

Temporal Dynamics of Land Use: Statistical Methods

OHD produces results that consist of a mean date with an SE of 30 y for each dateable object. (These dating outcomes, the details of their calculation, and the sampling procedures are described in the *SI Appendix* and refs. 41 and 42) The normally distributed individual-object probability distributions were combined to generate summed probability distributions (SPDs) for each study area, a method used by archaeologists to analyze radiocarbon dates from Rapa Nui (19) and elsewhere (see refs. 53 and 54 for reviews). Given a series of mean OHD dates with SEs, we derived a distribution by summing the fractions of date probability in any given year to get a measure of the equivalent number of dates, or density, assigned to that year. The summed probability fractions that form the curve indicate the periods when the obsidian artifacts most likely were created and, by proxy, the intensity of land use in different regions of the island from the first occupation until after European contact. Fig. 2 shows the OHD SPD curves for the three primary study areas.

The SPD curves cannot pinpoint events in history because a single flake in the dataset represents a range of probabilities for its exposure date, so its effect on the SPD curve is felt both before and after its true date of creation. Therefore, an environmental or social change that alters flake production in a given year will affect the SPD on either side of that year, with diminishing intensity in years farther away from (much earlier or later than) the true year of the event. This uncertainty tends to blur the relationship between changes in actual rates of tool production and the characteristics of an SPD curve.

To determine the point at which OHD samples actually began to decline, we used a curve-fitting method and compared the observed OHD SPDs with hypothetical distributions derived from land-use intensities and determined the best fits. These hypothetical trajectories were created by varying four parameters describing patterns of land-use change across a range of possibilities: (*i*) the rate of exponential growth in the production of datable obsidian before a decline (from 0.002 to 0.01 in increments of 0.002), (*ii*) the length of the plateau at which their production remains at its maximum (using 0, 25, 50, and 200 y), (*iii*) the year in which the creation of datable obsidian begins to decline from its maximum (from AD 1600–1850 in 5-y increments), and (*iv*) the constant exponential rate at which the creation of datable obsidian declines (from 0.002–0.1 in 0.002 increments and from 0.15–0.5 in 0.05 increments). These 59,160 hypothetical trajectories that depict a range of scenarios of obsidian discard were converted to OHD SPDs. We scaled these hypothetical SPDs to the maximum (after AD 1600) of each of the observed SPDs and found the best fit between models and observations using a least-squares method.

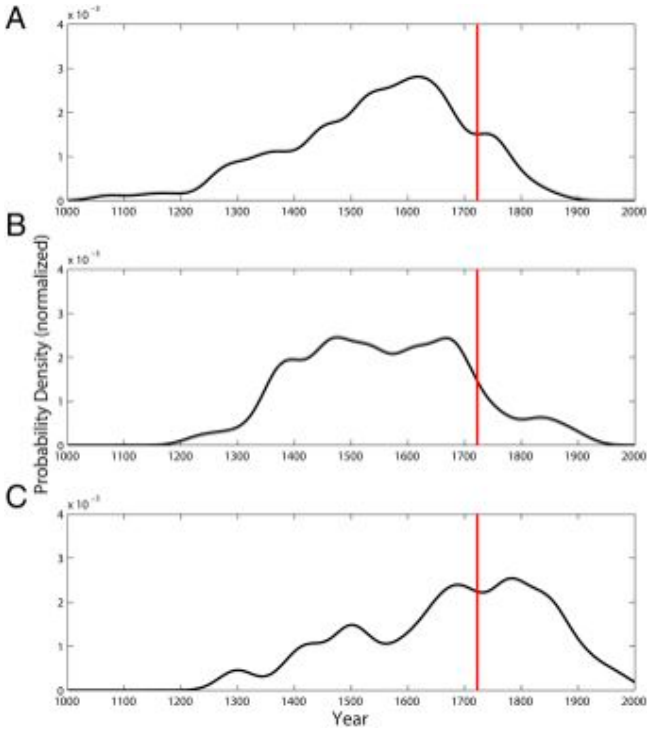

Fig. 2. OHD normalized SPD curves for SA1 (*A*), SA2 (*B*), and SA3 (*C*). The red line identifies the year AD 1722, the date of first European contact.

ANTHROPOLOGY

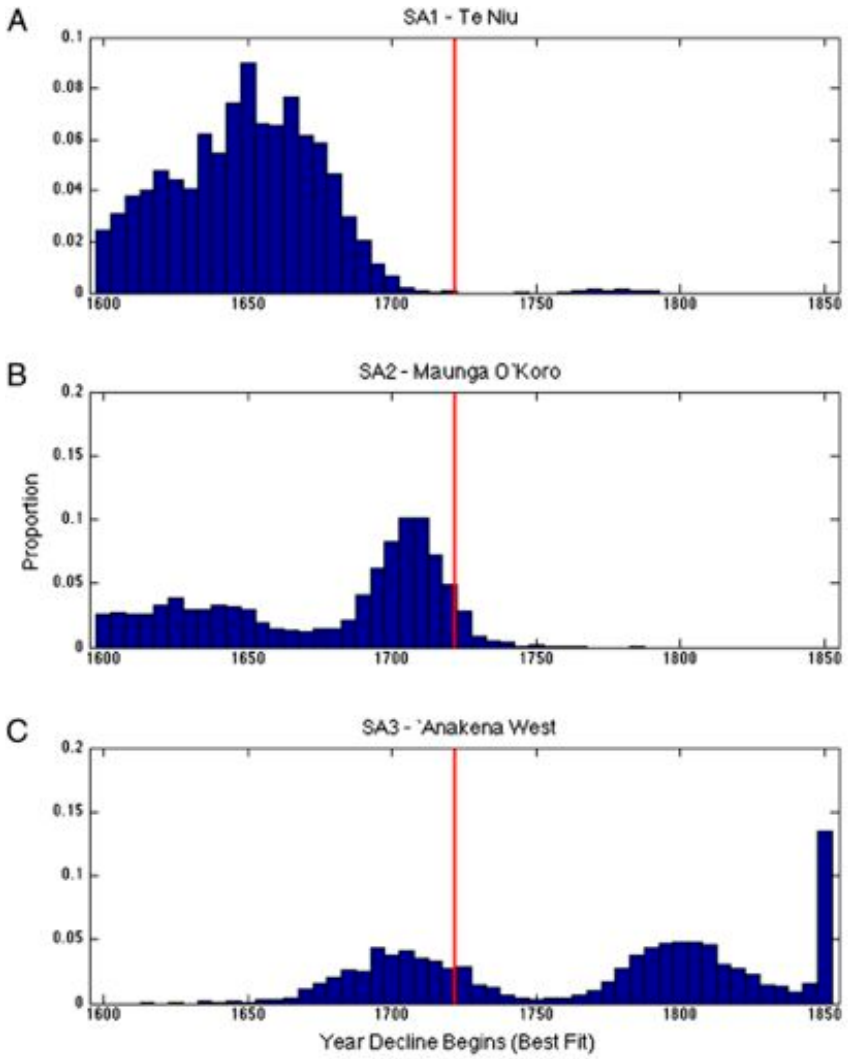

Fig. 3. The most likely date for the initiation of land-use decline in SA1 (*A*), SA2 (*B*), and SA3 (*C*). These normalized results are based on 2,500 bootstrap iterations of the OHD data at each study area. The red line identifies the year AD 1722, the date of first European contact.

The best fit was determined using three windows of comparison by minimizing the sum of the squared error across the spans of ±25, 50, and 75 y around the peak of the observed SPD. We focus on the ±50-y analytical window; the data for the other analytical windows are presented in *SI Appendix*, Fig. S2 and Table S4. This process yields a single estimate of the most likely date of the initiation of land-use decline in each study area. To assess the robustness of the findings, we bootstrapped (resampled with replacement) the distributions of mean OHD dates in each study area 2,500 times. By repeating the best-fit methodology using the resampled observed OHD SPDs, we determined distributions of dates of commencement of significant declines in the production of datable obsidian in each study area. Fig. 3 displays the histograms of the most likely year of decline commencement from the 2,500 bootstrap-and-fit iterations.

Our approach provides a robust means of determining when regions of the island were occupied and used and when the initial period of decline after AD 1600 began, including quantification of the uncertainty associated with these results. The degree of dispersion of best-fit years is a function of OHD sample size. Greater sample size would be expected to reduce the variability across the bootstrapped datasets and thus provide a more precise estimate of the actual point at which land-use decline begins by reducing the risk of small-pool sampling errors. This information on land-use change is related directly to regional food production, although differential behavioral strategies (e.g., horticultural, residential, and religious activities) in different study areas would influence the strength of the correlation. Changes in land use also should be connected to regional population, although that connection could be modulated further by differential behaviors.

Spatial Variation in the Dynamics of Land Use

The OHD SPD curve for SA1 near the coast on the northwest of the island indicates a steady increase in the intensity of land use from *ca*. AD 1220 to AD 1650 (Fig. 2*A*). The curve suggests land use peaked around AD 1650 and dropped rapidly thereafter. The best-fit curve methodology indicates that the most likely date for the initiation of land-use decline was *ca*. AD 1660, well before European contact in AD 1722 (Fig. 3*A*). Only 0.64% of iterations resulted in the decline beginning after AD 1720.

In the interior study area (SA2), land use initiated after AD 1200 with a rapid increase through the AD 1300s and a lower rate of increase until *ca*. AD 1480 (Fig. 2*B*). From that time land use remained relativity constant at a high level until the end of the AD 1600s. The best-fit curve methodology suggests that the most likely date of initial decline in the region was *ca*. AD 1705

or 1710 (Fig. 3*B*), indicating reduced intensity of use of upland regions just before European arrival on Rapa Nui. Of 2,500 iterations, 5.00% resulted in the decline beginning after AD 1720.

In contrast to SA1 and SA2, in the near coastal northeastern study area (SA3) land use increased at a relatively slower rate from *ca*. AD 1240 to *ca*. AD 1500, with a steeper increase during the AD 1600s to an initial peak around AD 1690 (Fig. 2*C*). From that time on there seems to be relatively constant land use until *ca*. AD 1800. The best-fit curve methodology suggests the most likely date for the initiation of land-use decline was *ca*. AD 1850 or later, well after European contact (Fig. 3*C*). We found 67.2% of iterations with a best-fit year of decline commencement after AD 1720.

Discussion

There is strong evidence for a decrease in the intensity of land use before European contact in two of the three primary study areas—the dry area of SA1 and the wet and infertile area of SA2. By the time of European contact, land use in both areas had declined by almost half. SA1 was at 53.7% of its AD 1618 maximum, and SA2 was at 60% of the post-AD 1600 maximum, which occurred in AD 1667. In the dry area of SA1 annual rainfall (*ca*. 805 mm) is close to the annual rainfall of 750 mm/y that has been identified as the lower boundary at which Hawaiian cultivators developed intensive dryland systems (46). We suggest that this area would have been highly vulnerable to periodic droughts and therefore would have been one of the earliest areas to be abandoned. In contrast, the central, upland portion of Rapa Nui (SA2 and surrounds) is wet but strikingly low in soil fertility in comparison with the lowlands of Rapa Nui (43). We suggest that cultivation of these poor soils could be sustained only through long-fallow shifting cultivation, and that attempting to farm the area with a shorter fallow cycle would have degraded the already very low fertility of this area. In contrast, SA3 represents a region with adequate rainfall and relatively fertile soils (Table 1). In this area, land use was relatively high during the late AD 1600s until after AD 1800. The individual OHD SPD curves of the three secondary study areas (SA4–6) yield less definitive temporal patterning (*SI Appendix*, Fig. S3) with lower confidence because of less intensive OHD sampling.

Our information demonstrates that some regions of Rapa Nui experienced declines in the intensity of land use before European contact. If that decrease in land use and associated food production was not offset by increased food production elsewhere on the island, then the results are consistent with a decrease in overall food supply before European contact. Information on population and soil fertility from more regions of Rapa Nui would be valuable, of course, but regional total food production could have declined (and influenced the dynamics of precontact society) with sustained production through European contact in some areas of the island.

Conclusion

New chronometric evidence from three study areas reveals spatial and temporal variation in Rapa Nui land use. Initial settlement and expansion occurred from *ca*. AD 1200, with the rapid development of the interior for agricultural activities beginning in the early AD 1300s. Reductions in the intensity of land use before European contact in the dry northwest section of Rapa Nui and the region of nutrient-leached soils in upland areas would have contributed to increasing land pressure in other parts of the island and may have led to periods of conflict as land use was renegotiated.

This temporal reconstruction of land-use history associated with food production argues against the notion of an island-wide precontact collapse as a useful explanatory concept for Rapa Nui—although it does support the reality of a precontact decline in land use that probably was associated with declines in food production. These results indicate that island-wide landscape use was modulated by an underlying climatic and biogeochemical matrix as well as by response to dynamic variations in climatic and biogeochemical factors. We propose that precontact declines in the intensity of land use (and presumably population) in dry and infertile regions of Rapa Nui better reflect a framework of environmental constraint than of environmental degradation—although constraint and degradation can intergrade, as in the case of infertile soils that are suitable for shifting cultivation being degraded through overuse.

ACKNOWLEDGMENTS. We thank the Consejo de Monumentos, Rapa Nui, and the Consejo de Monumentos Nacionales de Chile for permission to work on Easter Island; our island collaborators Ninoska Cuadros and the Corporación Nacional Forestal for assistance and support; Rod Wallace and Jen Huebert, University of Auckland, for the species identification of our carbon samples; Simon Bickler for sharing the Excel template he developed that calculates the summed probability distributions; and Mark Grote, University of California, Davis, for information on interpreting summed probability distributions. This work was funded by National Science Foundation Award BCS-0911056 with additional support from the National Geographic Society, the Earthwatch Institute, and the University of Auckland.

1. Hunt TL, Lipo CP (2006) Late colonization of Easter Island. *Science* 311(5767): 1603–1606.
2. Hunt TL, Lipo CP (2008) Evidence for a shorter chronology on Rapa Nui (Easter Island). *Journal of Island and Coastal Archaeology* 3(1):140–148.
3. Wilmshurst JM, Hunt TL, Lipo CP, Anderson AJ (2011) High-precision radiocarbon dating shows recent and rapid human colonization of East Polynesia. *Proc Natl Acad Sci USA* 108(5):1815–1820.
4. Mulrooney MA, Bickler SH, Allen MS, Ladefoged TN (2011) High-precision dating of colonization in East Polynesia. *Proc Natl Acad Sci USA* 108(23):E192–E194.
5. Metraux A (1940) *Ethnology of Easter Island*. Bernice Pauahi Bishop Museum Bulletin No. 160. (Bernice Pauahi Bishop Museum, Honolulu).
6. Heyerdahl T, Ferdon EN, Jr (1965) *The Archaeology of Easter Island: Reports of the Norwegian Archaeological Expedition to Easter Island and the East Pacific*. Monograph 24, Vol. 1. School for American Research and Museum of New Mexico, Santa Fe. (George Allen and Unwin Ltd., London).
7. Diamond JM (2005) *Collapse: How Societies Choose to Fail or Succeed* (Viking, New York).
8. Flenley JR, Bahn PG (2002) *The Enigmas of Easter Island: Island on the Edge* (Oxford Univ Press, Oxford, UK).
9. Kirch PV (1984) *The Evolution of Polynesian Chiefdoms* (Cambridge Univ Press, Cambridge, UK).
10. Lee G (1986) Easter Island rock art: Ideological symbols as evidence for socio-political change. PhD dissertation (University of California, Los Angeles, CA).
11. Van Tilburg J (1986) Power and symbol: The stylistic analysis of Easter Island monolithic sculpture. PhD dissertation (University of California, Los Angeles, CA).
12. Van Tilburg J (1994) *Easter Island: Archaeology, Ecology and Culture* (British Museum Press, London).
13. Vargas P, Cristino C, Izaurieta R (2006) *1000 Años en Rapa Nui. Arqueologia del Asentamiento* (Universidad de Chile, Santiago, Chile).
14. Stevenson CM (1984) Corporate descent group structure in Easter Island prehistory. PhD dissertation (Pennsylvania State University, State College, PA).
15. Stevenson CM (1986) The socio-political structure of the southern coastal area of Easter Island. *The Evolution of Island Societies*, ed Kirch PV (Cambridge Univ Press, Cambridge, UK), pp 69–77.
16. Stevenson CM, Haoa S (2008) *Prehistoric Rapa Nui.* Easter Island Foundation (Bearsville, Los Osos, CA).
17. Hunt TL, Lipo CP (2011) *The Statues that Walked: Unraveling the Mystery of Easter Island* (Free, New York).
18. Mulrooney MA (2012) Continuity or Collapse? Diachronic Settlement and Land Use in Hanga Ho'onu, Rapa Nui (Easter Island). PhD dissertation (University of Auckland, Auckland).
19. Mulrooney MA (2013) An island-wide assessment of the chronology of settlement and land use on Rapa Nui (Easter Island) based on radiocarbon data. *J Archaeol Sci* 40(12):4377–4399.
20. Mulrooney MA, Ladefoged TN, Stevenson CM, Haoa S (2010) Empirical assessment of a pre-European societal collapse on Rapa Nui (Easter Island). *The Gotland Papers: Selected Papers from the VII International Conference on Easter Island and the Pacific: Migration, Identity, and Cultural Heritage*, eds Wallin P, Martinsson-Wallin H (Gotland Univ Press, Gotland, Sweden), pp 141–154.
21. Rainbird P (2002) A message for our future? The Rapa Nui (Easter Island) ecodisaster and Pacific Island environments. *World Archaeol* 33(3):436–451.
22. Peiser B (2005) From genocide to ecocide, the rape of Rapa Nui. *Energy Environ* 16(3-4):513–539.
23. Kirch PV (2000) *On the Road of the Winds. An Archaeological History of the Pacific Islands before European Contact* (Univ of California Press, Berkeley, CA).

24. Stevenson CM (1997) *Archaeological Investigations on Easter Island, Maunga Tari: An Upland Agricultural Complex* (Easter Island Foundation, Bearsville and Cloudmountain, Los Osos, CA).
25. Routledge KP (1919) *The Mystery of Easter Island: The Story of an Expedition* (Sifton, Praed and Company, London).
26. Flenley JR (1993) The palaeoecology of Easter Island, and its ecological disaster. *Easter Island Studies: Contributions to the History of Rapanui in Memory of William T. Mulloy*, ed Fischer SR (Oxbow Books, Oxford, UK), pp 27–45.
27. Flenley JR (1996) Further evidence of vegetational change on Easter Island. *South Pacific Study* 16(2):135–141.
28. Flenley JR (1998) New data and new thoughts about Rapa Nui, in Easter Island. *Pacific Context South Seas Symposium: Proceedings of the Fourth International Conference on Easter Island and East Polynesia*, eds Stevenson CM, Lee G, Morin FJ (Easter Island Foundation, Los Osos, CA), pp 125–128.
29. Flenley JR, King SM (1984) Late Quaternary pollen records from Easter Island. *Nature* 307(5946):47–50.
30. Flenley JR, et al. (1991) The Late Quaternary vegetational and climatic history of Easter Island. *J Quaternary Sci* 6(2):85–115.
31. Flenley JR, Bahn PG (2007) Ratted out. *Am Sci* 95(1):4–5.
32. Hunt TL (2006) Rethinking the fall of Easter Island. *Am Sci* 94(5):412–419.
33. Hunt TL (2007) Rethinking Easter Island's ecological catastrophe. *J Archaeol Sci* 34(3): 485–502.
34. Mieth A, Bork H-R (2010) Humans, climate or introduced rats-which is to blame for the woodland destruction on prehistoric Rapa Nui (Easter Island)? *J Archaeol Sci* 37(2): 417–426.
35. Rull V, et al. (2010) Paleoecology of Easter Island: Evidence and uncertainties. *Earth Sci Rev* 99(1-2):50–60.
36. Mieth A, Bork H-R (2004) *Easter Island - Rapa Nui: Scientific Pathways to Secrets of the Past* (Christian-Albrechts-Universitat zu Kiel, Kiel, Germany).
37. Mann D, et al. (2008) Drought, vegetation change, and human history on Rapa Nui (Isla de Pascua, Easter Island). *Quat Res* 69(1):16–28.
38. Louwagie G, Stevenson CM, Langohr R (2006) Impact of moderate to marginal land suitability on prehistoric agricultural production and models of adaptive strategies for Easter Island (Rapa Nui), Chile. *J Anthropol Archaeol* 25(3):290–317.
39. Church F, Rigney J (1994) A microwear analysis of tools from Site 10-241, Easter Island – An inland processing site. *Rapa Nui Journal* 8(4):101–105.
40. Church F, Ellis JG (1996) A use-wear analysis of obsidian tools from an *ana kionga*. *Rapa Nui Journal* 10(4):81–88.
41. Stevenson CM, Novak SW (2011) Obsidian hydration dating by infrared spectroscopy: Method and calibration. *J Archaeol Sci* 38(7):1716–1726.
42. Stevenson CM, Ladefoged TN, Novak SW (2013) Prehistoric settlement on Rapa Nui, Chile: Obsidian hydration dating using infrared photoacoustic spectroscopy. *J Archaeol Sci* 40(7):3021–3030.
43. Vezzoli L, Acocella V (2009) Easter Island, SE Pacific: An end-member type of hotspot volcanism. *Geol Soc Am Bull* 121(5-6):869–886.
44. Ladefoged TN, Stevenson CM, Vitousek PM, Chadwick OA (2005) Soil nutrient depletion and the collapse of Rapa Nui society. *Rapa Nui Journal* 19(2):100–105.
45. Ladefoged TN, et al. (2010) Soil nutrient analysis of Rapa Nui gardening. *Archaeology in Oceania* 45(2):80–85.
46. Vitousek PM, et al. (2014) Farming the Rock: A biogeochemical perspective on intensive agriculture in Polynesia. *Journal of the Pacific Archaeology* 5(2):51–61.
47. Chadwick OA, et al. (2003) The impact of climate on the biogeochemical functioning of volcanic soils. *Chem Geol* 202(3-4):195–223.
48. Vitousek PM, et al. (2004) Agriculture, soils, and society in precontact Hawai'i. *Science* 304(5677):1665–1669.
49. Stevenson CM, Jackson T, Mieth A, Ladefoged TN (2006) Prehistoric agriculture at Maunga Orito, Easter Island (Rapa Nui), Chile. *Antiquity* 80(310):919–936.
50. Wallin P, Stevenson CM, Ladefoged TN (2005) Sweet Potato Production on Rapa Nui. *The Sweet Potato in the Oceania: A Reappraisal*, eds Ballard C, Brown P, Bourke RM, Harwood T (Ethnology Monographs, Pittsburgh, and Oceania Monographs, Sydney), pp 85–88.
51. Stevenson CM, Ladefoged TN, Haoa S (2002) Productive strategies in an uncertain environment: Prehistoric agriculture on Easter Island. *Rapa Nui Journal* 16(1):17–22.
52. Junk C, Claussen M (2011) Simulated climate variability in the region of Rapa Nui during the last millennium. *Climate of the Past* 7(2):579–586.
53. Bamforth DB, Grund B (2012) Radiocarbon calibration curves, summed probability distributions, and early Paleoindian population trends in North America. *J Archaeol Sci* 39(6):1768–1774.
54. Williams AN (2012) The use of summed radiocarbon probability distributions in archaeology: a review of methods. *J Archaeol Sci* 39(3):578–589.

Supplemental Information

Obsidian Hydration Dating Protocols

The obsidian samples used in this analysis were recovered from six systematically surveyed 500 x 500 m areas located throughout Rapa Nui (Fig. 1). These areas were selected to capture variation in prehistoric settlement patterns and agricultural field systems that may have been responsive to differences in rainfall, temperature, topography, and social processes. Close interval (5-10 m) pedestrian surface survey was used to record stone surface features (e.g., house patios, chicken houses, stacked-stone enclosures) and the distribution of prehistoric rock gardens within each study area. These features were surveyed with differential correction capable Trimble GPS hand-held units with sub-meter accuracy. Subsurface testing in gardens and adjacent to surface features was conducted by the excavation of 50 x 50 cm shovel tests. Each shovel test was excavated into the B-horizon and in many instances bedrock or decomposing bedrock was encountered at a depth of 50cm or less. The maximum depth excavation was 70cm. Obsidian debitage and carbon fragments were recovered during screening of the shovel test matrix and no samples were taken within 10 cm of the surface. Table S1 itemizes the number of dated obsidian artifacts by study area. This sample size reflects the use of all suitable materials that were recovered through excavation and the elimination of highly irregular items and artifacts with cracks and surface voids. Imperfections such these may trap moisture and lead to in inaccurate age determination.

Obsidian hydration dating was conducted by the senior author using infrared photoacoustic spectroscopy. The infrared response values were used to estimate diffused surface water (H_2O) concentrations which had accumulated since the creation of the artifact (i.e., the hydration layer). Age estimates were based upon laboratory developed calibrations that relate glass structural water (hydroxyl) to the rate of water diffusion at a specified temperature (1). This set of dating procedures was evaluated with two previously dated contexts; the early 13^{th} century deposits at Ahu Nau Nau on the north coast and a 19^{th} century planting pit from the west coast of the island. In each case the convergence between the Class 1 AMS dates and the obsidian hydration dates was strong as exhibited by numerous overlapping age ranges (2 S.D.) occurring within each context (2). This supports our current application of obsidian dating.

Obsidian hydration dating rate calibrations are temperature sensitive and the thermal history of the artifact is central to a reliable age determination. While many events and thermal contexts associated with the use-life of an obsidian artifact cannot be reconstructed, it is assumed that this period is very short prior to entry into the archaeological record. Once discarded and buried, it is possible to monitor the temperature history over the course of an annual cycle to estimate an effective hydration temperature.

Columns of ground temperature sensors were buried at nine locations around Rapa Nui at coastal and inland elevations. HOBO digital loggers were buried at 10 cm, 25 cm, and 50 cm in open stone-free areas and within the boundaries of adjacent rock gardens (Table

S2). The purpose of this dual placement was to see how surface rock cover impacted the below-ground temperatures. Ground temperature was recorded each 1.5 hours over the course of one year. Upon recovery, the data were downloaded and a mean annual temperature was calculated. These data were converted to an effective hydration temperature suitable to an exponential process such as water diffusion in glass using the procedures outlined in Stevenson et al. (2).

Effective hydration temperatures ranged between 21-23^{o}C for each of the columns and no patterned temperature differences were found between open areas and rock gardens. Three exceptions to this general range were noted. The coolest ground temperatures (19-20^{o}C) occurred at Rano Oroi which is located near the summit of Rapa Nui at an elevation of 450 m above sea level. High wind and rainfall levels are coupled to lower air temperatures. At the other end of the continuum, the warmest ground temperatures (24-25^{o}C) were registered by the sensor at ‘Anakena. We attribute this to the high level of calcareous sand in the sediment that raise overall thermal diffusivity. Cool ground temperatures near 20^{o}C were also recorded in a small cave formed from a collapsed lava tube. In our dating of obsidian artifacts from all locations, we applied the effective hydration temperature for the 25 cm depth within each study area to the artifacts recovered from that study area.

Table S1: Processed obsidian hydration dating samples by study area.

Study Area	No. of Sites	No. of Test Units	No. of Obsidian Dates
SA 1 (Te Niu)	8	10	127
SA 2 (Maunga O’koro)	12	12	79
SA 3 (‘Anakena West)	11	11	80
SA 4 (Hiva Hiva-coastal)	8	8	33
SA 5 (Hiva Hiva-inland)	15	15	53
SA 6 (Maunga Pui)	5	6	56
Total			428

Table S2: Soil temperatures and computed effective hydration temperatures for Rapa Nui. See Fig. 1, Appendix 1 for sensor locations 1-8.

				Mean ºC			EHT ºC	
Location	**Context**	**Date**	**10cm**	**25cm**	**50cm**	**10cm**	**25cm**	**50cm**
1A.Te Niu (SA1)	Set 1	4/7/09-4/7/10	20.74	20.71	20.70	21.27	21.10	21.07
1B.Te Niu (SA1)	Set 2	4/7/09-4/7/10	22.15	22.17	22.05	22.84	22.62	22.31
1B.Te Niu (SA1)	Set 3	4/7/09-4/7/10	21.93	22.07	22.01	22.45	22.45	22.30
1A.Te Niu (SA1)	Set 4	4/7/09-4/7/10	21.17	21.29	21.23	21.75	21.75	21.61
2.‘Anakena (SA3)	Set 1	8/10/10-8/10/11	24.27	24.09	23.80	25.18	24.81	24.27
3.O’Koro (SA2)	Set 1	3/26/10-3/23/11	21.15	21.11	20.78	22.00	21.80	21.20
3.O’Koro (SA2)	Set 2	3/26/10-3/23/11	21.38	21.12	20.82	22.28	21.72	21.22
4.Rano Oroi	Set 1	4/2/10-3/23/11	19.51	19.13	18.82	20.11	19.50	19.03
5.South Coast	Set 1	8/7/10-8/7/11	22.66	22.46	------	23.69	23.26	------
5.South Coast	Set 2	8/7/10-8/7/11	22.77	22.62	22.21	23.68	23.35	22.72
6.Anamarama	Set 4	5/6/10-5/6/11	22.38	22.44	22.31	23.33	23.13	22.78
	Set 6	5/5/10-5/5/11	22.36	22.22	22.17	23.27	22.93	22.71
7.Hiva Hiva (SA4)	Set 1	9/25/07-9/24/08	22.63 (15cm)		22.21 (40cm)			22.47 (40cm)
8.Cave, Hiva Hiva	Set 2	10/10/07-/24/08	19.85 (0cm)			20.1 (0cm)		

Figure S1: The location of digital soil temperature sensors placed on Rapa Nui between 2008 and 2011.

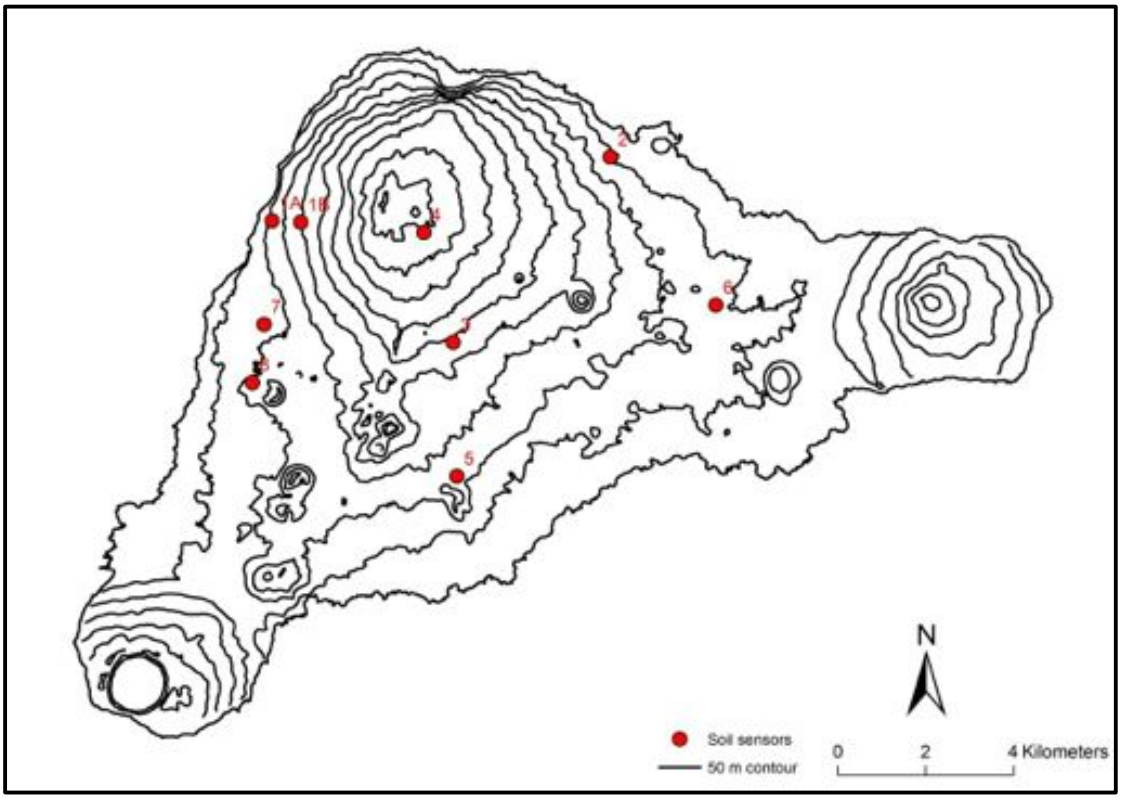

Projecting Spatial Variation of Rainfall

We derived spatial projections of mean annual rainfall using a combination of data from six high-resolution HOBO weather stations placed across the island and long-run data from Mataveri Airport near the town of Hanga Roa. The relatively short series of rainfall data (spanning less than three years) from the HOBO stations was compared to the daily records at the airport. We derived a function to describe the relationship between daily rainfall at each HOBO location and the airport series where data for both points were available. We then used this relationship to generate a 62-year sequence at each HOBO site, projecting from the airport series. These six series were used to estimate a "precipitation lapse rate," or the linear relationship between precipitation amounts and elevation, for the island. In the absence of data in the drier areas in the lee of the strong easterly winds we estimated a rain shadow effect as a function of topography, working from the pattern observed at the Kohala Peninsula on the Island of Hawai'i.

Table S3: Secondary study areas with corresponding distance to coast, elevation and rainfall values (measurements taken at center of 500 x 500 m quadrant).

Survey Area	**Distance to coast (m)**	**Elevation (m)**	**Rainfall (mm)**
(SA4) coastal Hiva Hiva	329	51	1330
(SA5) inland Hiva Hiva	1874	129	1465
(SA6) Maunga Pui	3208	126	1461

Table S4: Best-fit land usage trajectories to observed (not resampled) OHD data.

Best fit (smallest error) by site and "span" (window of evaluation) in years ± crash															
	SA1	SA2	SA3	SA1	SA2	SA3	SA1	SA2	SA3	SA1	SA2	SA3	SA1	SA2	SA3
Span	25	25	25	50	50	50	75	75	75	100	100	100	150	150	150
Crash year	1665	1710	1820	1660	1705	1825	1650	1700	1845	1645	1700	1850	1665	1685	1840
Decline rate	0.018	0.04	0.006	0.014	0.028	0.008	0.01	0.022	0.016	0.008	0.02	0.018	0.01	0.014	0.014
Sum squared error	3.40E-08	7.28E-08	1.97E-08	2.09E-07	3.50E-07	7.89E-08	1.07E-06	1.01E-06	3.04E-07	4.32E-06	2.83E-06	1.02E-06	1.53E-05	1.11E-05	4.75E-06
Avg annual SSE	6.80E-10	1.46E-09	3.94E-10	2.09E-09	3.50E-09	7.89E-10	7.11E-09	6.72E-09	2.03E-09	2.16E-08	1.42E-08	5.09E-09	5.12E-08	3.69E-08	1.58E-08
Parameter ranges tested:															
Crash year	every 5 years from 1600 to 1850														
Decline rate	0 to 0.1 in 0.002 increments and 0.15 to 0.5 in 0.05 increments														
Span	25, 50, 75, 100, 150 years before and after the crash date being tested														
Best fit when crash date is constrained to 1722 and only decline rate is being altered to maximize fit															
	SA1	SA2	SA3	SA1	SA2	SA3	SA1	SA2	SA3	SA1	SA2	SA3	SA1	SA2	SA3
Span	25	25	25	50	50	50	75	75	75	100	100	100	150	150	150
Crash year	1722	1722	1722	1722	1722	1722	1722	1722	1722	1722	1722	1722	1722	1722	1722
Decline rate	0.15	0.088	0.008	0.044	0.058	0.002	0.03	0.044	0	0.028	0.036	0	0.026	0.026	0.002
Sum squared error	1.10E-05	3.75E-07	5.42E-07	3.57E-05	2.20E-06	3.00E-06	4.44E-05	5.44E-06	8.08E-06	4.62E-05	1.10E-05	2.18E-05	4.75E-05	2.81E-05	0.00010189
Avg annual SSE	2.19E-07	7.50E-09	1.08E-08	3.57E-07	2.20E-08	3.00E-08	2.96E-07	3.62E-08	5.39E-08	2.31E-07	5.52E-08	1.09E-07	1.58E-07	9.37E-08	3.40E-07

Figure S2: One of the 2,500 bootstrapped summed probability distribution curves (shown in black). Overlaid are 4 of the 59,160 hypothetical trajectories, with the best-fit curve (shown in blue) and three alternatives (shown in gray). The best fit parameters are AD 1695 (begin decline), rise rate of 0.004, plateau of 50 years, decline rate of 0.01. The peak of black line (bootstrapped SPD) is AD 1663. The red lines indicate the extremes of the ±50 year window of comparison, or span over which the fit is determined.

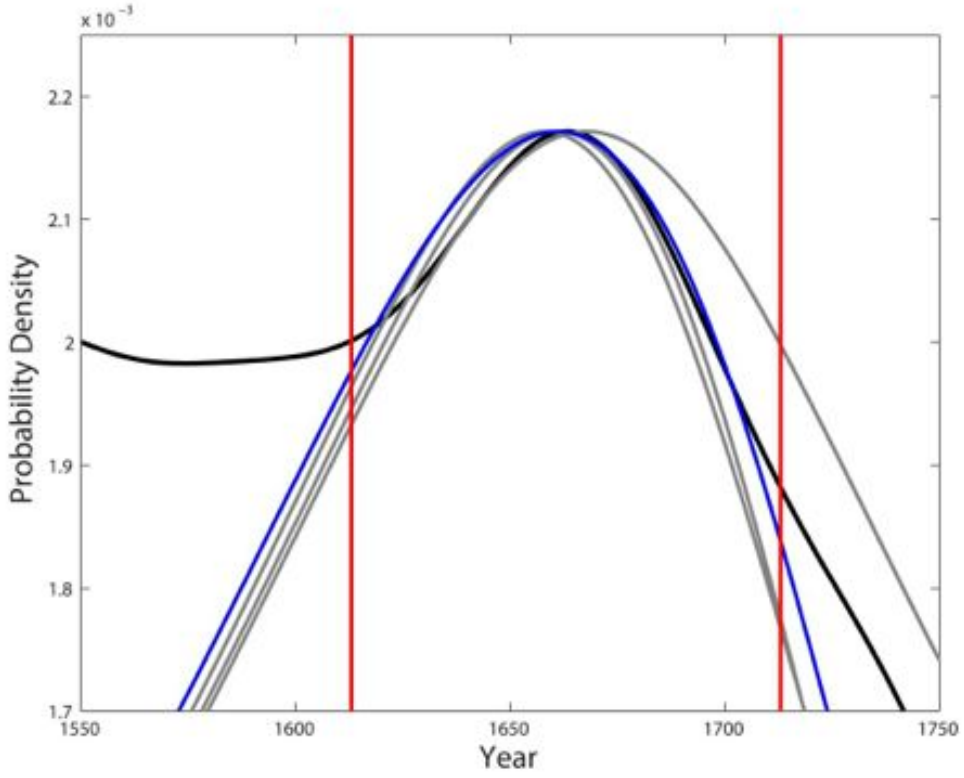

Figure S3: OHD summed probability distribution (SPD) curves for A) SA1; B) SA2; C) SA3, D) SA4; E) SA5; and F) SA6. The curves are normalized so that the area beneath each sums to 1. The red line identifies the year AD 1722, the date of European contact.

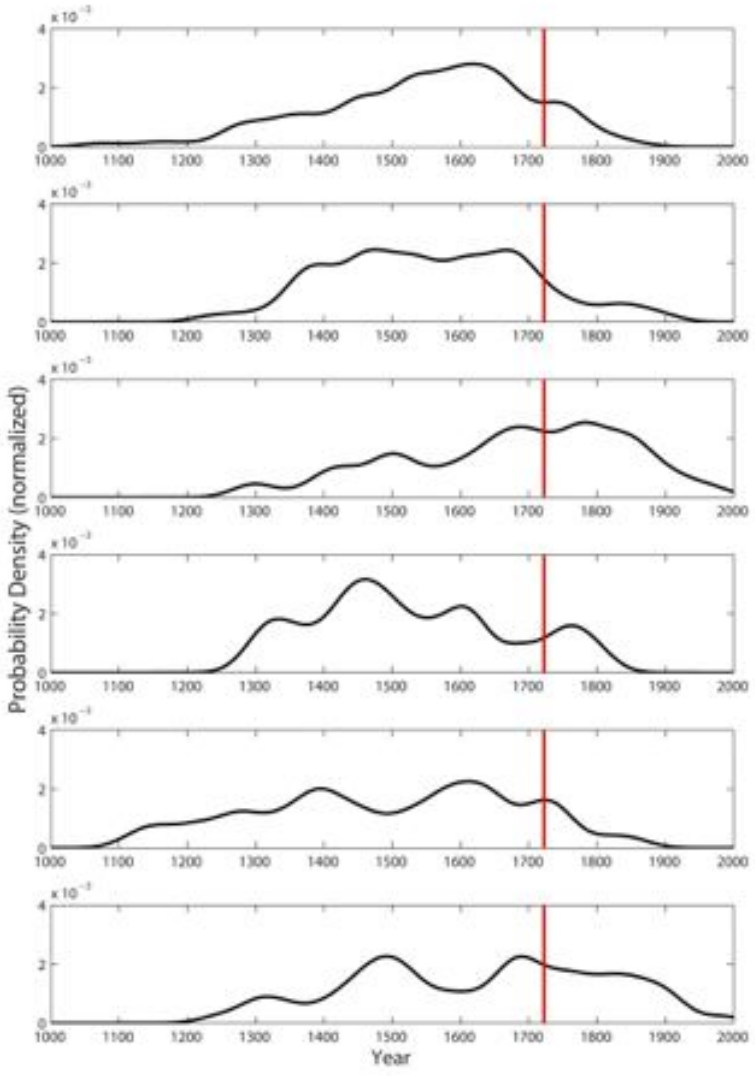

References

1. Stevenson CM, Novak SW (2011) Obsidian hydration dating by infrared spectroscopy: Method and calibration. *Journal of Archaeological Science* 38:1716-1726.

2. Stevenson CM, Ladefoged TN, Novak SW (2013) Prehistoric settlement on Rapa Nui, Chile: Obsidian hydration dating using infrared photoacoustic spectroscopy. *Journal of Archaeological Science* 40:3021-3030.